

# The efficiency of “viscous interaction” between the solar wind and the magnetosphere during intense northward IMF events

Bruce T. Tsurutani

Jet Propulsion Laboratory, California Institute of Technology, Pasadena, California

W. D. Gonzalez

Instituto de Pesquisas Espaciais, Sao Jose Dos Campos, Sao Paulo, Brazil

**Abstract.** We examined 11 cases when the interplanetary magnetic field (IMF) was intensely northward ( $> 10$  nT) for long durations of time ( $> 3$  hours), to quantitatively determine an upper limit on the efficiency of solar wind energy injection into the magnetosphere. We have specifically selected these large  $B_N$  events to minimize the effects of magnetic reconnection. Many of these cases occurred during intervals of high-speed streams associated with coronal mass ejections when viscous interaction effects might be at a maximum. It is found that the typical efficiency of solar wind energy injection into the magnetosphere is  $1.0 \times 10^{-3}$  to  $4.0 \times 10^{-3}$ , 100 to 30 times less efficient than during periods of intense southward IMFs. Other energy sinks not included in these numbers are discussed. Estimates of their magnitudes are provided.

## Introduction

It has recently been suggested [Tsurutani et al., 1992a] that the efficiency of solar wind energy input into the Earth's magnetosphere via viscous interaction [Axford and Hines, 1961] is quite low,  $\sim 1.2 \times 10^{-3}$ . The interval used for illustration was an intense northward IMF event within the famous August 1972 high speed solar wind stream. The coupling efficiency during this interval was almost two orders of magnitude below that during magnetic reconnection intervals such as those causing intense substorms and storms. If this result is true in general, then it can be concluded that viscous interaction processes (such as the Kelvin-Helmholtz instability on the flanks of the magnetopause/magnetotail [Tamao, 1965; Chen and Hasegawa, 1979; Southwood, 1974]) may not be of primary importance for direct solar wind energy injection into the magnetosphere. Delayed energy injection (after storage in the magnetotail) may be possible, but from the 1972 event results, it appears that it would have to be delayed by at least five hours or more.

Although the above example shows that this one high speed solar wind stream led to geomagnetic quiet during part of the complex interplanetary event, the study has the inherent difficulty that the interplanetary spacecraft (Pioneer 10) was at a large distance from Earth (2.2 AU) and at a slightly different solar longitude, requiring calculations of radial and coronation delays to match the spacecraft and Earth event times. Because it is difficult to make general conclusions from this single case, further analyses are needed.

The purpose of this paper is to study eleven more examples. We use (ISEE-3) intervals where the IMF had very large

northward components ( $>10$  nT) for long durations ( $> 3$  hours) of time. The events have been previously listed in part by Gonzalez and Tsurutani [1987], for other purposes. These interplanetary events were taken from 1978-1979, when a complete and continuous ISEE-3 interplanetary plasma and field data set existed.

## Results

Figure 1 is an example of a  $B_N$  event where  $B_N$  is greater than 10 nT for over three hours. From top to bottom are the proton temperature, solar wind velocity, density,  $B_Y$  and  $B_Z$  (in GSE coordinates), B magnitude and ground based AE and  $D_{ST}$  indices. The intense  $B_N$  event occurs at 15-21 UT November 11, 1979. The peak  $B_N$  value of 20 nT occurs at 18 UT, coincident with the peak B magnitude of -23 nT. Note the exceptionally low AE values and a slightly positive  $D_{ST}$  index during the event.

The  $B_N$  event is associated with a moderate speed solar wind stream. An interplanetary fast forward shock occurs at -0130 UT November 11. This is indicated by the abrupt increase in proton temperature, solar wind velocity and density and magnetic field magnitude at this time.

Table 1 gives the solar wind, magnetospheric and ionospheric parameters for the 11  $B_N$  events. The columns from the left are: 1) the date and time (the listed time is the midpoint of the  $B_N$  event), 2) the peak  $B_N$  intensity in nT, 3) the duration of the  $B_N$  event, 4) the peak magnetic field magnitude, 5) the average AE of the event, and 6) the average  $D_{ST}$  during the event. In the latter column, R stands for storm recovery phase and Q is a quiet day. Column 7) is the solar wind velocity, 8) the proton density in nucleons/cm<sup>3</sup>, 9) the helium density, and 10) the  $B_Y$  component in GSE coordinates. When there are two values of  $B_Y$  given,  $B_Y$  was variable during the event, and the two most representative values are listed. These intense  $B_N$  events were often associated with CME-related high speed streams, similar to the previously reported August 1972 event [Tsurutani et al., 1992a]. These events were located in either the sheath region behind the shock or in the driver gas proper. A more detailed discussion can be found in Tsurutani et al. [1988; 1992 b].

From the above measurements, we will calculate the solar wind energy flux incident upon the magnetosphere, the amount of energy deposited in the magnetosphere/ionosphere at typical auroral and lower latitudes, and finally the efficiency of energy injection. We will lead the reader through these straightforward steps.

First, we assume pressure balance at the magnetopause [Spreiter et al., 1966]:

$$k\rho V_{sw}^2 \cos^2 \theta = \frac{(fB)^2}{8\pi} \quad (1)$$

where the ram pressure (left-side of equation) is balanced by the magnetic pressure (right-side). In this expression,  $\rho$  is the total proton plus helium mass density,  $V_{sw}$  the solar wind velocity,  $\theta$  the angle that  $V_{sw}$  makes relative to the magnetopause normal, and B the magnetopause magnetic field. The value  $k$  represents the degree of specular reflection (2.0 is maximum for an elastic collision) and  $f$  the magnetic field intensification factor due to the Chapman-Ferraro current. It has been empirically shown that  $f^2/k \sim 1.69$  [Holzer and Slavin, 1978] a number we will use in our estimations.

In Table 2, we have used the measured values of Table 1 to calculate the value  $(p_p + p_{He}) V_{sw}^2$  (column 1). The magnetopause field strength (at the nose) necessary to balance the solar wind ram pressure is calculated using equation 1 (column 2), and the magnetopause stand-off distance in Earth-radii determined by assuming that the magnetopause field strength at its nose is twice the uncompressed dipolar strength (column 3).

*Sibeck et al.* [1991] found that the field expansion factor of the dawn meridian magnetopause distance relative to the subsolar distance for large  $B_N$  values is -1.1. This factor was determined empirically for northward IMF B values between +4 and +6 nT. We have used this factor in calculating the cross-sectional area (column 4) of the magnetosphere (a conservative estimate).

Column 5 is the incident solar wind energy flux in  $\text{erg cm}^{-2}\text{s}^{-1}$  and column 6 is the total energy impinging on the dayside magnetosphere, i.e., the values in column 4 times those in column 5.

A commonly used expression for the energy dissipation within the magnetosphere [Akasofu, 1981] as applied to typical aurora and lower latitudes, is:

$$U_T = U_O + U_A + U_J \quad (2)$$

where  $U_J$  and  $U_A$  are the ring current and auroral energies, and  $U_O$  the rate of Joule heating. The Joule heating rate has been approximated by  $2 \times 10^5 \text{ AE (nT) ergs s}^{-1}$  and the auroral particle energy by  $1 \times 10^{15} \text{ AE (nT) ergs s}^{-1}$  [Akasofu, 1981]. The value  $U_J$  is given by  $4 \times 10^{20} (dD_{ST}/dt + D_{ST}/\tau) \text{ erg s}^{-1}$  with  $D_{ST}$  given in nT. Here  $\tau$  is -10 hrs, the average ring current decay time. Baumjohann and Kamide [1984] have shown that Joule heating is linearly proportional to AE throughout the range of AE: 200 nT to 1000 nT, the specific range of interest here.

From Table 1, it is noted that there is no discernible ring current energy injection for any of these events. Thus, we take  $U_O = 0$  for these cases.  $U_A + U_J$  can be approximated as equal to  $3 \times 10^{15} \text{ AE (nT) erg s}^{-1}$ .  $U_T$  has been calculated using the above relationships for each of the 11 events and is given as column 1 of Table 3. The energy deposition in the magnetosphere relative to the total solar wind energy flux impinging upon the magnetosphere, e.g., the efficiency of energy transfer, is given in column 2. The latter values are relatively constant. For 9 of 11 events, the efficiency varies from  $1.0 \times 10^{-3}$  to  $4.0 \times 10^{-3}$ . One event had an energy efficiency that was anomalously low,  $7.1 \times 10^{-4}$  on 29-30 May 1979. Another event had an efficiency that was anomalously high. This is on October 7, 1980 with an apparent efficiency of  $1.1 \times 10^{-2}$ .

The IMF By value is listed in the last column of Table 1. On the supposition that magnetic reconnection could still take place if By is large (during  $B_N$  events), we compared the solar wind energy input efficiency to that of the sign and magnitude of the IMF By. No obvious correlations are apparent.

The above expression in (2) does not include energy deposition at high (polar cap) latitudes, however. It is well known that the auroral oval shrinks during  $B_N$  events and it is possible that some energy deposition occurs poleward of the AE stations ( $>68^\circ \text{ MLAT}$ ). Makita et al. [1988], following the work of Meng [1981], have examined polar particle precipitation during strong interplanetary  $B_N$  intervals. They find that the entire polar region is often filled with "burst-type soft electron precipitations". From the figures of Makita et al., [1988], we find a flux between  $10^{-2}$  to  $10^0 \text{ erg cm}^{-2}\text{ster}^{-1}$ . Integrating from  $68^\circ$  to  $85^\circ$  magnetic

latitude, we determine a polar cap size of  $3.5 \times 10^{17} \text{ cm}^2$ . Thus, the energy flux is  $-4.4 \times 10^{16}$  to  $4.4 \times 10^{17} \text{ erg S}^{-1}$  over the two polar caps. Although the lower energy flux limit is negligible in comparison to the numbers in Table 2, we note that the upper energy limit is comparable to the aurora zone plus ring current energy fluxes derived from the Akasofu [1981] expression. Thus, there should be an uncertainty factor of -2 associated with our solar wind-magnetosphere coupling efficiencies, due to polar cap precipitation.

High latitude Joule heating is another magnetospheric/ionosphere energy sink that could be missed by the energy expression, equation (2). There are indications that there can be significant high latitude polar cap potentials during intense interplanetary  $B_N$  intervals [Heelis and Coley, 1992; Freeman *et al.*, 1993]. However, J. Fuller-Rowell [personal communication, 1994] has indicated that the ratio of the energy associated with Joule heating to that of particle precipitation will be no more than a factor of 2-3 for the polar cap during large IMF  $B_N$  events, a factor of -2 being a typical number.

## Discussion

In this work we have examined eleven intense, long-duration ( $>3$  hours)  $B_N$  events to estimate the solar wind coupling efficiency to the magnetosphere. For most of the 11 events, we find relatively constant values, only varying by a factor of 3. No obvious solar wind features are present which account for this slight variability, if it is real. It should be noted that the numbers (and efficiencies) given in Table 3 maybe low by a factor of 4 if the polar cap precipitation reaches a level of  $10^3 \text{ ergs cm}^{-2} \text{ s}^{-1} \text{ ster}^{-1}$  and Joule heating is twice this value. However, since this precipitation level and Joule heating rate are only upper limits, the values in Table 3 should give reasonable estimates.

The initial idea of a viscous-like interaction between the solar wind (magnetosheath) and the magnetosphere/magnetotail was first presented by Axford and Hines [1961]. Since that time several attempts have been made to determine the specific mechanism of interaction and to try to bound the limits of its energy efficiency. Sonnerup [1980] considered a purely viscous model which had no current limitation effects. He determined a potential drop across the boundary layers to be only 10-15% of the total potential drop across the magnetosphere. Eastman and Hones [1970] and Sckopke *et al.* [1981] experimentally arrived at 5-25 kV potentials across the boundary layers (see review by Cowley [1982]), a small fraction of the total cross-magnetospheric potential drop, in agreement with Sonnerup's model. Mozer [1984], from 28 magnetopause crossings near local dusk, determined the dusk-to-dawn potential drops were only a few kV and concluded that this potential was less than 10% of the total magnetospheric electric potential. Baumjohann and Haerendel [1986] demonstrated that viscous interaction plays only a "minor role" for equatorial convection at  $L = 6.6$ . However, more recently, [Freeman *et al.*, 1993] have calculated a 60-80 kV potential drop across the polar cap during an intense northward IMF event.

Even though the potential drops across the boundary layers appear to be somewhat bounded (most estimates give small potential drops), it is still difficult to derive an energy flux because of the lack of a quantitative knowledge of the current systems in these regions. If we make a very simplistic assumption that viscous interaction is - 10% as efficient as

magnetic reconnection and 10% of the solar wind energy flux gets into the magnetosphere during magnetic storms, this implies that viscous interaction could provide 1% of the solar wind energy to the magnetosphere/magnetotail. The numbers presented in this paper are lower than this value, and hence are consistent with this overall picture.

Another type of solar wind energy transfer mechanism suggested by Sonnerup [1980] is cross-field diffusion by resonant wave-particle interactions at the dayside magnetopause [Tsurutani and Thorne, 1982; Gendrin, 1983]. The ultimate energy source for the broadband ELF/VLF waves must be the solar wind/magnetosphere interaction. It has been suggested that these wave-particle interactions are responsible for the dayside aurora [Tsurutani et al., 1981; Thorne and Tsurutani, 1991]. The latter has an intensity of  $\sim 1.0 \text{ erg cm}^{-2} \text{ s}^{-1}$  [Eather, private comm., 1981]. Assuming a latitudinal width of  $\sim 1.0$  degree (100 km) for the precipitation region and a precipitation latitude of  $65^\circ$ , one derives an energy deposition rate of  $\sim 10^{16} \text{ ergs s}^{-1}$  over the two auroral zones. This number represents about 0.01% of the solar wind ram energy flux, or only 1070 of the energy dissipated in the magnetosphere during intense  $B_n$  events.

The above numbers give an estimate of the energy injection efficiency during intense IMF  $B_n$  events. It should be noted that magnetic reconnection in the cusp regions and associated, localized, polar cap potential drops are possible [Reiff et al., 1981], so these numbers are thus only an upper limit to the efficiency of viscous interaction (and also of reconnection). We have seen that the sum of UT, polar cap precipitation and Joule heating are equal to or less than 1% of the solar wind energy flux. It will be quite useful to know how much energy is lost down the tail [see Owen and Slavin, 1992] and how much Joule heating occurs over the polar cap to refine this estimate further. For the latter problem, we will examine the TIROS data in the near future.

**Acknowledgments.** We wish to thank C.I. Meng, V. Vasyliunas and I. Fuller-Rowell for very helpful scientific discussions concerning this work. Portions of this work were carried out at the Jet Propulsion Laboratory, California Institute of Technology, under contract with the National Aeronautics and Space Administration. We kindly acknowledge grant TPWRAAJ0334.

## References

- Akasofu, S. I., Energy coupling between the solar wind and the magnetosphere, *Space Sci. Rev.*, 28, 121, 1981.
- Axford, W. I. and C. O. Hines, A unifying theory of high-latitude geophysical phenomena and geomagnetic storms, *Can. J. Phys.*, 39, 1433, 1961.
- Baumjohann, W. and Y. Kamide, Hemispherical Joule heating and the AE indices, *J. Geophys. Res.*, 89, 383, 1984.
- Baumjohann, W. and G. Haerendel, Dayside convection, viscous interaction and magnetic merging, *Solar-Wind-Magnetosphere Coupling*, ed. Y. Kamide and J. A. Slavin, Terra Sci., Tokyo, 415, 1986.
- Chen, L. and A. Hasegawa, A theory of long-period magnetic pulsations. I., Steady state excitation of field-line resonances, *J. Geophys. Res.*, 79, 1024, 1974.
- Cowley, S. W. H., The causes of convection in the Earth's magnetosphere: A review of developments during the IMS, *Rev. Geophys. Space Phys.*, 20, 531, 1982.

- Eastman, I. E. and E. W. Hones, Jr., The magnetopause layer and plasma boundary layer of the magnetosphere, in *Quantitative Modeling of Mag. Processes*, Geophys. Mon. Ser. 21, edited by W. P. Olson, AGU, Washington, D. C., 401, 1979.
- Freeman, M. P., C. J. Farrugia, L. F. Burlaga, M. R. Hairston, M. E. Greenspan, J. M. Ruohoniemi, and R. P. Lepping, The interaction of a magnetic cloud with the Earth: Ionospheric convection in the northern and southern hemisphere for a wide range of quasi-steady interplanetary magnetic field conditions, *J. Geophys. Res.*, 98, 7633, 1993.
- Heelis, R. A. and W. R. Coley, East-west ion drifts at mid-latitudes observed by Dynamics Explorer 2, *J. Geophys. Res.*, 97, 19401, 1992.
- Gendrin, R., Magnetic turbulence and diffusion processes in the magnetopause boundary layer, *Geophys. Res. Lett.*, 10, 769, 1983.
- Gonzalez, W. D. and B. T. Tsurutani, Criteria of interplanetary parameters causing intense magnetic storms ( $D_{ST} < -100$  nT), *Planet. Space Sci.*, 35, 1101, 1987.
- Holzer, R. E. and J. A. Slavin, Magnetic flux transfer associated with expansions and contractions of the dayside magnetosphere, *J. Geophys. Res.*, 83, 3831, 1978.
- Makita, K., C. I. Meng and S. I. Akasofu, Latitudinal electron precipitation patterns during large and small IMF magnitudes for northward IMF conditions, *J. Geophys. Res.*, 93, 97, 1988.
- Meng, C. I., Polar cap arcs and the plasma sheet, *Geophys. Res. Lett.*, 8, 273, 1981.
- Mozer, F. S., Electric field evidence on the viscous interaction at the magnetopause, *Geophys. Res. Lett.*, 11, 135, 1984.
- Owen, C. J. and J. A. Slavin, Viscously driven plasma flows in the deep geomagnetic tail, *Geophys. Res. Lett.*, 19, 1443, 1992.
- Riciff, P., R. W. Spiro and T. W. Hill, Dependence of polar cap potential drop on interplanetary parameters, *J. Geophys. Res.*, 86, 739, 1981.
- Sckopke, N., External plasma flows, in *Msg. Bound. Layers, ESA SP-148*, ed. B. Battrock, ESA, Noordwijk, Holland, 37, 1979.
- Sibeck, D. G., R. E. Lopez and E. C. Roelof, Solar wind control of the magnetopause shape, location and motion, *J. Geophys. Res.*, 96, 5489, 1991.
- Sonnerup, B. U. O., Theory of the low latitude boundary layer, *J. Geophys. Res.*, 85, 2017, 1980.
- Southwood, D. J., Some features of field-line resonance in the magnetosphere, *Planet. Space Sci.*, 22, 483, 1974.
- Spreiter, J. R., A. L. Summers, and A. Y. Alksne, Hydrodynamic flow around the magnetosphere, *Planet. Space Sci.*, 14, 223, 1966.
- Tamao, T., Transmission and coupling resonance of hydromagnetic disturbances in the non-uniform Earth's magnetosphere, *Sci. Rep., Tohoku Univ., Ser. 5.*, 17, 43, 1965.
- Thorne, R. M. and B. T. Tsurutani, Wave-particle interactions in the magnetopause boundary layer, in *Physics of Space Plasmas (1990)* ed. by T. Chang et al., Sci Publ. Inc., Cambridge, Mass., 10, 119, 1991.
- Tsurutani, B. T., E. J. Smith, R. M. Thorne et al., Wave particle interactions at the magnetopause: contributions to the dayside aurora, *Geophys. Res. Lett.*, 8, 183, 1981.
- Tsurutani, B. T. and R. M. Thorne, Diffusion processes in the magnetopause boundary layer, *Geophys. Res. Lett.*, 9, 1247, 1982.
- Tsurutani, B. T., W. D. Gonzalez, F. Tang, S. I. Akasofu, and E. J. Smith, Origins of interplanetary southward energetic fields

responsible for major magnetic storms near solar maximum (1978-1979), *J. Geophys. Res.*, 93, 8519, 1988.

Tsurutani, B. T., W. D. Gonzalez, F. Tang, Y. T. Lee, M. Okada and D. Park, Reply to L. J. Lanzerotti: Solar wind ram pressure corrections and an estimation of the efficiency of viscous interaction, *Geophys. Res. Lett.*, 19, 1993, 1992a.

Tsurutani, B. T., W. D. Gonzalez, F. Tang and Y. T. Lee, Great magnetic storms, *Geophys. Res. Lett.*, 19, 73, 1992b.

---

B. T. Tsurutani, Jet Propulsion Laboratory, California Institute of Technology, Pasadena, CA 91109. (e-mail: btsurutani@jplsp.jpl.nasa.gov)

W. D. Gonzalez, Instituto de Pesquisas Espaciais, Sao Paulo, Brazil. (e-mail: gonzalez@das.inpe.br)

(Received September 28, 1994; revised November 11, 1994; accepted December 16, 1994.)

---

Copyright 1994 by the American Geophysical Union.

Paper number

0148-0227/94/94GL-2034M\$05.00

**Figure 1.** An example of a  $B_N$  event, from 15-21 UT, November 11, 1979.  $B_N$  is  $\geq 10$  nT, and reaches a peak value of 20 nT at 18 UT.  $B_y$  is large and variable during the interval. This event is associated with a moderate speed solar wind stream. No driver gas is evident.

Figure 1. An example of a  $B_N$  event, from 15-21 UT, November 11, 1979.  $B_N$  is  $\geq 10$  nT, and reaches a peak value of 20 nT at 18 UT.  $B_y$  is large and variable during the interval. This event is associated with a moderate speed solar wind stream. No driver gas is evident.

TSURUTANI ET AL. VISCIOUS INTERACTION EFFICIENCY

TSURUTANI ET AL. VISCIOUS INTERACTION EFFICIENCY

TSURUTANI ET AL. VISCIOUS INTERACTION EFFICIENCY

TSURUTANI ET AL. VISCIOUS INTERACTION EFFICIENCY

TSURUTANI ET AL. VISCIOUS INTERACTION EFFICIENCY

TSURUTANI ET AL. VISCIOUS INTERACTION EFFICIENCY

TSURUTANI ET AL. VISCIOUS INTERACTION EFFICIENCY

TSURUTANI ET AL. VISCIOUS INTERACTION EFFICIENCY

TSURUTANI ET AL. VISCIOUS INTERACTION EFFICIENCY

TSURUTANI ET AL. VISCIOUS INTERACTION EFFICIENCY

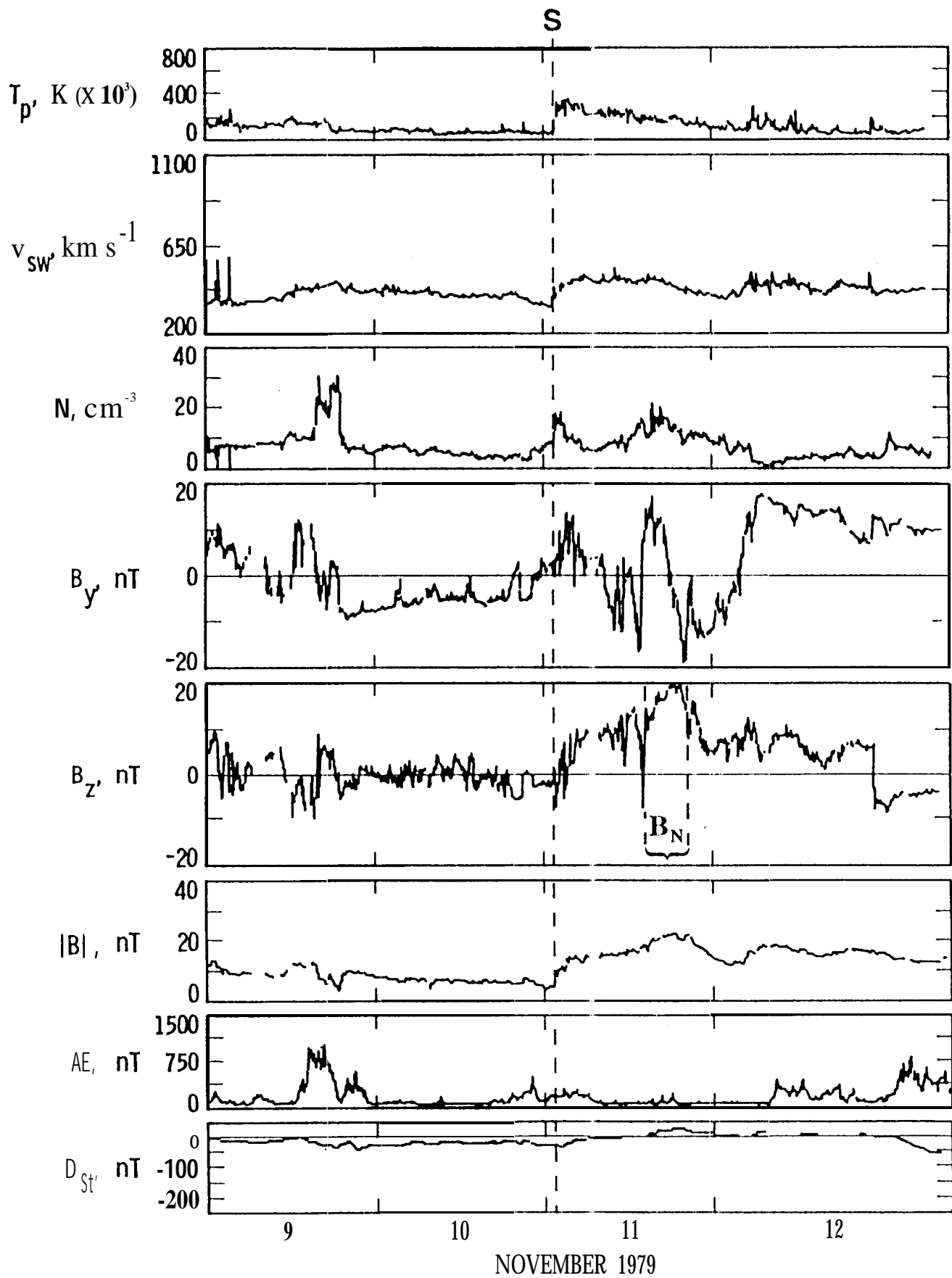




Table 1. Interplanetary and Magnetospheric Parameters for the  $B_N$  Events

Date (U.T.)	Peak $B_N$ (nT)	Duration (h)	Peak $ B $ (nT)	$\Delta E$ (nT)	$D_{ST}$ (nT)	$v$ (km s <sup>-1</sup> )	$\rho_p$ (n cm <sup>-3</sup> )	$\rho_{He}$ (n cm <sup>-3</sup> )	$B_y$ (nT)
1. 1X December 1978 (0100)	15	3	26	175	0	450	10.0	0.8	-12,+14
2. 21 February 1979 (1200)	20	4	22	75	R	560	12.0	0.4	+22
3. 3 April (1230)	12	3	14	75	R	440	8.0	0.4	-4
4. 5 April (0300)	20	4	33	200	R	605	11.0	1.0	-10,+20
5. 5 April (1230)	30	4	40	300	0	695	15.0	1.1	-8,+18
6. 29-30 May (2130)	15	3	23	150	0+	750	20.0	1.0	+8
7. 20 August (0830)	18	6	30	150	0+	670	13.0	0.4	25,+5
8. 18-19 September (2400)	12	3	15	35	R(Q)	365	12.0	0.8	+6.5
9. 6 October (1800)	18	3	20	110	R	370	45.0	2.0	+10,-10
10. 7 October (0800)	16	4	20	350	R	425	12.0	0.2	+4
11. 11 November (1800)	20	6	23	100	0+	450	12.0	0.8	+12,-10

Table 2. Calculated Interplanetary and Magnetospheric Parameters

	$(\rho_{\text{H}} + \rho_{\text{He}}) v_{\text{sw}}^2$ ( $\text{g cm}^{-1} \text{s}^{-2}$ )	$B_{\text{mp}}$ (Gauss)	$R_{\text{SO}}$ ( $R_{\text{E}}$ : 6380 km)	Area ( $\text{cm}^2$ )	$1/2 MN v_{\text{sw}}^3$ ( $\text{erg cm}^{-2} \text{s}^{-1}$ )	$E_{\text{T}}$ ( $\text{ergs-l}$ )
1.	$4.5 \times 10^{-8}$	$8.2 \times 10^{-4}$	9.0	$1.3 \times 10^{20}$	1.0	$1.3 \times 10^{20}$
2.	$7.1 \times 10^{-8}$	$1.0 \times 10^{-3}$	8.4	$1.1 \times 10^{20}$	2.0	$2.2 \times 10^{20}$
7	$3.1 \times 10^{-8}$	$6.8 \times 10^{-4}$	9.6	$1.4 \times 10^{20}$	0.7	$1.0 \times 10^{20}$
4.	$9.2 \times 10^{-8}$	$1.2 \times 10^{-3}$	7.9	$7.0 \times 10^{19}$	2.8	$2.0 \times 10^{20}$
5.	$1.6 \times 10^{-7}$	$1.5 \times 10^{-7}$	7.3	$8.2 \times 10^{19}$	5.4	$4.4 \times 10^{20}$
6.	$2.7 \times 10^{-7}$	$1.8 \times 10^{-3}$	6.9	$7.4 \times 10^{19}$	8.5	$6.7 \times 10^{20}$
7.	$1.1 \times 10^{-7}$	$1.3 \times 10^{-3}$	7.7	$9.2 \times 10^{19}$	3.7	$1.3 \times 10^{20}$
8.	$3.4 \times 10^{-8}$	$7.1 \times 10^{-4}$	9.5	$1.4 \times 10^{20}$	0.6	$8.4 \times 10^{19}$
9.	$1.2 \times 10^{-7}$	$1.2 \times 10^{-3}$	7.7	$9.2 \times 10^{19}$	2.2	$2.0 \times 10^{20}$
10.	$3.9 \times 10^{-8}$	$7.6 \times 10^{-4}$	9.2	$1.3 \times 10^{20}$	0.8	$1.0 \times 10^{20}$
11.	$5.1 \times 10^{-8}$	$8.7 \times 10^{-4}$	8.8	$1.2 \times 10^{20}$	1.2	$1.4 \times 10^{20}$

Table 3.  $U_T$  and Energy Transfer Efficiency

	$dE_{mag}/dt$ $erg\ s^{-1}$	$\eta$ efficiency
1.	$5.3 \times 10^{17}$	$4.0 \times 10^{-3}$
2.	$2.2 \times 10^{17}$	$1.0 \times 10^{-3}$
3	$2.2 \times 10^{17}$	$2.2 \times 10^{-3}$
4.	$6.0 \times 10^{17}$	$3.0 \times 10^{-3}$
5.	$9.0 \times 10^{17}$	$2.0 \times 10^{-3}$
6.	$4.5 \times 10^{17}$	$7.1 \times 10^{-4}$
7.	$4.5 \times 10^{17}$	$3.4 \times 10^{-3}$
8.	$1.4 \times 10^{17}$	$1.3 \times 10^{-3}$
9.	$3.3 \times 10^{17}$	$1.7 \times 10^{-3}$
[0.	$1.1 \times 10^{18}$	$1. \times 10^{-2}$
11.	$3.0 \times 10^{17}$	$2.1 \times 10^{-3}$